Parasitic nematode fatty acid- and retinol-binding proteins compromise host immunity by interfering with host lipid signaling pathways

Sophia C. Parks[1], Chau Nguyen[1], Shyon Nasrolahi[1,5], Damian Juncaj[1], Dihong Lu[1], Raghavendran Ramaswamy[2], Harpal Dhillon[1], Anna Buchman[3], Omar S. Akbari[3], Naoki Yamanaka[4], Martin J. Boulanger[2], and Adler R. Dillman[1*]

[1]Department of Nematology, University of California, Riverside, California, 92521, USA.
[2]Department of Biochemistry and Microbiology, University of Victoria, BC, Canada V8P 5C2
[3]Division of Biological Sciences, Section of Cell and Developmental Biology, University of California, San Diego, La Jolla, California, 92093, USA.
[4]Department of Entomology, University of California, Riverside, California, 92521, USA.
[5]Present address: Keck School of Medicine, University of Southern California, Los Angeles California, 90033, USA.
* Corresponding: adlerd@ucr.edu

Graphical Abstract

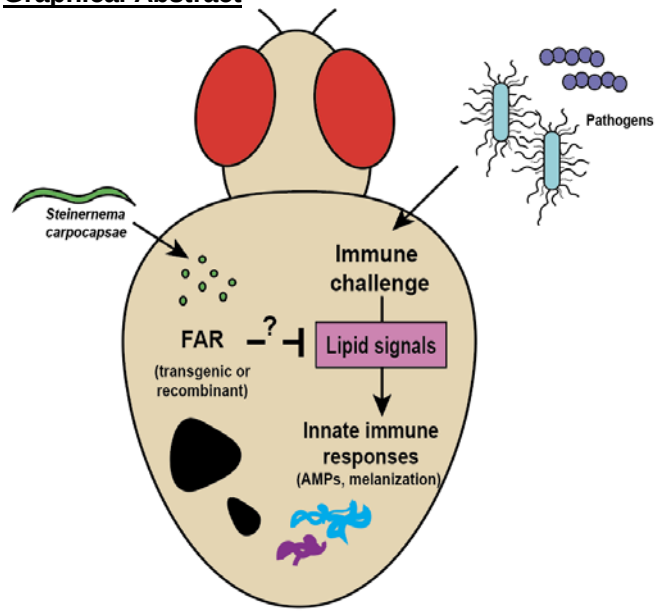

Abstract

Parasitic nematodes cause significant morbidity and mortality globally. Excretory/secretory products (ESPs) such as fatty acid- and retinol- binding proteins (FARs) are hypothesized to suppress host immunity during infection, yet little is known about their interactions with host tissues. Leveraging the insect parasitic nematode, *Steinernema carpocapsae*, we provide the first *in vivo* study that shows FARs modulate animal immunity, causing an increase in susceptibility to bacterial infection. Next we determined that FARs dampen various aspects of the fly immune response including the phenoloxidase cascade and antimicrobial peptide (AMP) production. Finally, we found that FARs deplete lipid signaling precursors *in vivo* as well as bind to these fatty acids *in vitro,* suggesting that FARs elicit their immunomodulatory effects by altering the availability of lipid signaling molecules necessary for a functional immune response. Collectively, these data reveal a complex role for FARs in immunosuppression and provide detailed mechanistic insight into parasitism in phylum Nematoda.

Significance

A central aspect of parasitic nematode success is their ability to modify host biology, including evasion and/or subversion of host immunity. Modulation of host biology and the pathology caused by parasitic nematodes is largely effected through the release of proteins and small molecules. There are hundreds of proteins released by nematodes during an infection and few have been studied in detail. Fatty acid- and retinol-binding proteins (FARs) are a unique protein family released during infection. We report that nematode FARs from *S. carpocapsae*, *C. elegans* and *A. ceylanicum* dampen fly immunity decreasing

resistance to infection. Mechanistically, this is achieved through modulation of the phenoloxidase cascade and antimicrobial peptide production. Furthermore, FARs alter the availability of lipid immune signaling precursors *in vivo* and show binding specificity *in vitro*.

Introduction

Helminths continue to cause significant morbidity and mortality on a global scale through human disease, sickening of livestock, and a reduction in crop yield (Hotez et al., 2014; Pullan et al., 2014). Parasitic nematodes are responsible for significant human suffering with a striking 1.5 billion people infected with soil-transmitted helminths alone (WHO, 2020). Much of the nematodes' success in parasitism is due to their ability to disguise themselves from host immune defenses. Little is understood about the mechanisms that underpin these stealth processes. Increasing our understanding of immune modulation by parasitic nematodes could inform treatment of such infections and lead to therapeutics for immune dysregulation such as autoimmune disorders.

Protein and small-molecule effectors seem to be crucial for parasites to successfully infect plants, invertebrates, and vertebrate hosts (Cooper and Eleftherianos, 2016; Shepherd et al., 2015). Upon infecting their hosts, nematodes release ESPs into surrounding tissues, which are the primary point of interaction between the parasite and host and are hypothesized to aid in nematode survival and cause damage to the host. A variety of proteins are found in nematode ESPs, some of which are known to cause tissue damage and modulate host immunity. One unique family of proteins released by parasitic nematodes, is the fatty acid- and retinol-binding proteins. FARs are small (~20 kDa), alpha-helix rich, and are likely to be responsible for sequestering essential lipids required for reproduction and development (Kennedy et al., 2013). FARs were first discovered in the filarial nematode *Onchocerca volvulus*, the causative agent of river blindness. FARs have subsequently been identified in the free-living nematode *Caenorhabditis elegans* as well as several other nematode parasites of animals, plants and insects (Sani, 1985; Kennedy, 1995; Kennedy, 1997). In *C. elegans*, FARs are localized in the hypodermis, head and lips which are regularly in contact with the outside environment, as well as the excretory cell connected to the hypodermis (Jordanova et al., 2009).

FARs attracted attention because they were shown to be secreted by parasitic nematodes and are strongly immunogenic in infected hosts (Garofalo et al., 2002; Kennedy et al., 1995a; Kennedy et al., 1995b; Zhan et al., 2018). Moreover, several studies also suggest that FAR proteins modulate plant immunity. The strongest evidence comes from a study on a FAR protein from the plant-parasitic nematode *Meloidogyne javanica*, which, when expressed *in planta*, has been shown to increase the host susceptibility to further infection (Iberkleid et al., 2013). FARs are released by infectious-stage parasites, and therefore several studies have suggested the importance of FARs in facilitating parasitism by sequestering host retinol and/or fatty acids interfering with or suppressing immunity (Bradley et al., 2001; Ramanathan et al., 2011). It is hypothesized that FARs also modulate animal immunity, yet no studies have investigated this experimentally. The functional role of these proteins in animal hosts as well as the mechanism of action behind these functions remains unknown.

One of the challenges to studying these host-parasite interactions is the paucity of studies in model systems to develop testable hypotheses about effector function during infection. Using an insect-parasitic nematode model allows studies to be conducted on large populations and some insect-parasitic nematode species are closely related to vertebrate-parasitic species, leading to insights that may be directly applicable to mammalian diseases (Hallem et al., 2007; Ward, 2015). Entomopathogenic nematodes (EPNs) are parasites of insects that are related to skin-penetrating nematodes of mammals such as *Strongyloides stercoralis* (Ciche, 2007; Dillman et al., 2015; Lok, 2007). Using the EPN *Steinernema carpocapsae* as a model parasite and the fruit fly *Drosophila melanogaster* as a model host may facilitate a mechanistic understanding of effectors such as FARs. The fruit fly is a powerful genetic model with a complex innate immune system containing mechanisms conserved in mammals (Troha and Buchon, 2019). The *D. melanogaster* immune response has been a fruitful model for mammalian immunity and is divided into two innate response types; cellular and humoral immunity (Hoffmann et al., 1999b; Lemaitre and Hoffmann, 2007). Furthermore, immune responses are generally activated by two main NF-kB signaling pathways, Toll and Imd, similar to human toll-like receptors (TLR) and tumor necrosis factor (TNF) signaling respectively (Hoffmann et al., 1999a). The Toll and Imd pathways are activated by different pathogens, depending on properties such as cell wall constituents. The cellular response is carried out by hemocytes and involves processes that surround and kill the invading pathogen including phagocytosis and encapsulation, whereas the humoral response involves the

generation of antimicrobial peptides (AMPs) by the fat body, analogous to the mammalian liver and adipose tissues, which are small, cationic and often amphipathic peptides that function as endogenous antimicrobials that "mop up" pathogens left over from the cellular immune defense system by disrupting negatively charged microbial membranes. Systemic production of AMPs is controlled by the two NF-kB pathways, Toll and Imd (Lemaitre and Hoffmann, 2007 Hanson, 2019). A combinatorial response by the innate immune system is likely elicited during a nematode infection (Castillo et al., 2011).

In this study, we tested the hypothesis that nematode FAR proteins (Sc-FARs) have the ability to dampen the animal immune response (*D. melanogaster*) in the context of various bacterial infections. Significant immune suppression by FARs was observed resulting in decreased host survival to bacterial infections, accompanied by a significant increase in microbe growth. To understand how Sc-FARs modulate host immunity several readouts of *Drosophila* immunity were assessed including AMP production and phenoloxidase activity. Potential FAR binding partners were assessed using metabolomics and *in vitro* protein-metabolite interactions. These data led us to propose a model for nematode FAR modulation of host immunity.

Results

Genomic analysis of S. carpocapsae revealed a presence of novel FAR proteins.

Analysis of the genome sequence of the generalist insect-parasitic nematode *S. carpocapsae* revealed an expansion of FARs compared to other nematodes (Dillman et al., 2015). We evaluated the presence of FARs in a variety of parasitic nematodes and *C. elegans* and found a dynamic range of putative FAR-encoding genes among nematode genomes (Table 1). We found that *S. carpocapsae* had the most with 45 putative FAR proteins, compared to 9 in *C. elegans*, 16 in *S. stercoralis* and 5 in *Ascaris lumbricoides* (Table 1). While FARs are thought to be essential for lipid sequestration, we found no putative FAR-encoding genes in either *T. spiralis* or *T. muris*, suggesting that either these nematodes have divergent putative FAR genes that were not recognizable by sequence similarity, or that they have evolved a different strategy to acquire lipids from their hosts. Of the 45 putative FARs in *S. carpocapsae*, five FARs were found in the ESPs of an *in vitro* infection model (Lu et al., 2017). We chose the two found in highest abundance, Sc-FAR-1 (L596_023208) and Sc-FAR-2 (L596_016036), for further study.

Nematode FAR proteins modulate host immunity decreasing resistance to bacterial pathogens.

To investigate the immunomodulatory effects of FARs, we used *D. melanogaster* as a model host and the two most abundant ESP-derived *S. carpocapsae* FARs Sc-FAR-1 and Sc-FAR-2, hereafter referred to as FAR-1 and FAR-2 respectively. To measure immune modulation by these FARs, we first determined the LD_{30} dose of the Gram-positive, extracellular pathogen, *Streptococcus pneumoniae* in OregonR flies and established the appropriate dose for injection and the baseline outcome of infections at this dose (Figure S1). The outcome of infection was assessed using fly survival and microbial growth over time. We found that the LD_{30} (the dose that kills 30% of adult flies in the first 2-7 days post infection) is the optimal dose for injection, since it provides enough sensitivity to detect shifts in the outcome of infection. Recombinant Sc-FAR-1 and Sc-FAR-2 were co-injected into adult flies, mimicking an EPN infection with delivery of the protein and pathogenic bacteria into the hemocoel. A one-time dose of FAR-1 or FAR-2 co-injected with the LD_{30} dose of *S. pneumoniae* significantly affects the outcome of bacterial infection in flies. A dose-dependent effect was observed where a high dose (250 ng) decreased host survival while lower doses did not elicit the same effect (Figures 1A and 1B). We measured microbe growth over time for FAR-2 recombinant injections due to its dose-dependent spread of effects on the outcome of survival. A trend in increased microbial load was also observed, where the flies injected with the highest dose of FAR had a greater number of bacterial cells 24-hours post-injection (Figure 1C). Heat-denatured recombinant FAR-1 or FAR-2 was co-injected at the highest dose tested (250 ng); no difference was observed when compared to *S. pneumoniae*-only injected flies, confirming that the addition of recombinant FAR in a one-time dose affects the flies' ability to deal with pathogenic infection (Figure S2).

In addition to a one-time injection of recombinant of FAR-1 and FAR-2, we also determined the outcome of infection using transgenic flies expressing either FAR-1 or FAR-2. We ectopically expressed these FARs in flies using the Gal4/UAS system and confirmed with Western blot (Figures S3 and S4). We also evaluated the effects of *C. elegans*-derived FAR-8 and a FAR from the human hookworm *A. ceylanicum* (Figure S5). Flies expressing nematode FAR proteins in the fat body, hemocytes, and salivary glands are healthy and have a normal lifespan (Figure S5). An expression-dependent decrease in survival was observed with strong, ubiquitous expression resulting in the most severe decrease in

survival. Expression of FARs only in the hemocytes had the least severe effect on the outcome of infection (Figure 2A). The effect observed on survival is specific to FAR-expressing flies since their genetic control did not elicit the same effect (Figure S6). FAR-expressing flies also displayed a significant increase in microbial load 24 hours post-injection (Figure 2B). To determine whether this effect was pathogen-specific, the Gram-negative EPN symbiont *Xenorhabdus innexi*, one of the least virulent bacteria in the genus, was also injected to induce an immune response (Kim et al., 2017). Similar to *S. pneumoniae* infection alone, flies expressing FAR-1 had a significant decrease in survival for both doses, whereas FAR-2-expressing flies were only affected when injected with the higher dose (Figure 2C). CFUs were also measured post-injection. A significant increase in microbial load was observed in both FAR-1 & 2-expressing flies (Figure 2D). The intracellular Gram-positive pathogen *Listeria monocytogenes* was also tested. We found FAR expressing flies to have the same decrease in survival, however there was no significant difference in microbe load 24 hours post-injection (Figures 2E and 2F). These data demonstrate that FARs significantly affect the outcome of a bacterial infection, in a dose dependent manner, by decreasing survival post infection and dampening the ability of the flies to control the bacterial growth over time. Interestingly, flies expressing *C. elegans* FAR-8 and a FAR from the human hookworm *A. ceylanicum* showed a similar immune deficient phenotype when challenged with an *S. pneumoniae* infection (Figure S7). This suggests that the immunomodulatory effects of FARs are conserved across taxa, solidifying the value of this model for understanding the mechanism of FARs in parasitic infection.

FARs dampen multiple aspects of immunity in D. melanogaster

D. melanogaster has a sophisticated, evolutionarily conserved, innate immune response that can be categorized into two main branches: a systemic humoral response, and a cellular response mainly carried out by various types of hemocytes (Figure S8). To establish the mechanism by which FAR-1 and FAR-2 elicit their immunomodulatory effects, we evaluated several readouts of immunity including phenoloxidase activity and melanization, which are essential immune defenses during a bacterial infection. Disseminated melanization and PO activity was measured post-injection with *L. monocytogenes*, which elicits a robust disseminated melanization phenotype 4 days post injected (Ayres and Schneider, 2008). Flies expressing FAR-1 and FAR-2 showed a significant decrease in survival when injected with ~1,000 CFUs of *L. monocytogenes* (Fig 2E). After injection with 1,000 cells of *L. monocytogenes*, FAR-1 and FAR-2 expressing flies were unable to initiate PO activity six hours post-infection (Figure 3A). Similarly, disseminated melanization, measured as two or more melanization spots throughout the body, was reduced to only 20%, from 60% in controls, of the population in FAR-expressing flies 4 days post-injection (Figure 3B). To further investigate the effect of FARs on innate immunity we assessed their involvement in the production of AMPs. We performed RT-qPCR to measure expression levels of two AMP-encoding genes: *Defensin*, mostly regulated by the Imd pathway, and *Drosomycin*, mostly regulated by the Toll pathway (Hanson et al., 2019). After infection with *S. pneumonia*, both FAR-1 and -2 expressing flies exhibit at least a 14-fold reduction in the AMP response for both *Drosomycin* and *Defensin* (Figure 3C).

FARs alter in vivo fatty acid availability including putative immune signaling molecules.

To determine the molecular mechanism underlying the immunomodulatory effects of FAR-1 and FAR-2, we initially screened for potential metabolites available to FAR using an untargeted metabolomics approach. We found many phosphatidylcholines (PC), phosphatidylethanolamines (PE), as well as multiple fatty acids that were less abundant in FAR-expressing flies, suggesting they are somehow depleted by FARs (Figure S9). Since many of the molecules that were significantly altered were unclassified, we moved to a targeted metabolomics approach. During an infection, FARs are excreted into the host tissue and may remain in circulation to elicit their immunomodulatory effects. Therefore, we proceeded to test differences in lipid metabolite abundance in the hemolymph of the FAR-1-expressing and control flies. Hemolymph was collected from 200 male flies and lipid concentrations between groups were assessed with targeted metabolomics. We found that several fatty acid metabolites including both 9(10)-EpOME and 12(13)-EpOME, which are epoxide derivatives of linoleic acid and leukotoxins in mammals, were significantly lower in FAR-1-expressing flies when compared to the genetic control. 13-HODE and arachidonic acid were also significantly reduced in FAR- expressing flies (Figure 4). We anticipate that FAR-2 would cause similar reductions in the fatty acids and alterations to the fly's lipid metabolite profile.

FAR binding specificity in vitro.

To determine potential binding partners of FARs, we measured the binding affinity to various fatty acids and retinol *in vitro*. Initially, we determined the binding affinity of both Sc FARs to the 11-(Dansylamino) undecanoic acid (DAUDA), and retinol, by calculating the equilibrium dissociation constant (Kd) (Figures S10A, B and S11AB). We found the Kd to be in the 1-10 µM range (Figures S10C, D and S11C, D). Using DAUDA as the fluorophore, we tested various fatty acids in 10-fold excess in competition with DAUDA to determine preferred fatty acid binding partners for FARs *in vitro*. When FAR binds to a fatty acid in this assay, DAUDA is displaced from the protein resulting in a reduction in peak fluorescence intensity (Figures S10E, F). Linoleic acid caused the greatest displacement of DAUDA and 9(10)- and 12(13)-EpOME disrupted DAUDA bound to FAR-2 greater than FAR-1 (Figure 5). The results indicated that FAR-1 & 2 have measurable differences in binding specificity, suggesting that they may target different lipid signaling molecules during infection.

Discussion

Understanding how parasitic nematodes circumvent host immune responses has significant potential to inform therapeutic intervention strategies. Much of what is known about FAR proteins and their potential interactions with host immunity comes from *in vitro* studies (Bath et al., 2009; Fairfax et al., 2014; Fairfax et al., 2009; Rey-Burusco et al., 2014; Rey-Burusco et al., 2015). FARs initially attracted attention because they are excreted by parasitic nematodes during an active infection and elicit a host immune response (Garofalo et al., 2002; Kennedy et al., 1995a; Kennedy et al., 1995b; Zhan et al., 2018). Here we provide the first *in vivo* study in an animal system along with evidence demonstrating that FARs alter the animal immune response. We found that the outcomes of bacterial infections are significantly worse in flies when FARs are present.

We have investigated the specific aspects of immunity that are affected by FARs, and found modulation of various mechanisms including phenoloxidase activity, a key mechanism to control invading parasites, and antimicrobial peptide production. Upon injury or infection, insects rapidly initiate the melanization cascade leading to deposition of melanin along the wounding site and around invading microbes or pathogens. This serves to block invading pathogens, prevent excess hemolymph loss, and to encapsulate and kill pathogens with reactive oxygen species (ROS) and other toxins. Melanization is independent of the classical immune pathways (Toll & Imd). Rather, it is dependent upon activation of prophenoloxidase (proPO), which is a proenzyme that is cleaved by prophenoloxidase activating enzyme (PPAE) to its active form phenoloxidase (PO). Phenoloxidase is the catalyst for the oxidation of mono- and diphenols to orthoquinones, which form polymers with melanin non-enzymatically, during which ROS is produced (Cooper et al., 2019; Lemaitre and Hoffmann, 2007). Since the family of FAR proteins is highly conserved among many nematode species it is important to understand whether FARs elicit their immunomodulatory effects in similar ways (Table 1). Slight differences between the effects of the two Sc-FARs are apparent in flies challenged with *X. innexi*, where FAR-2 expressing flies given a 25,000 CFU dose did not do significantly worse than the control flies, as well as the recombinant studies and AMP production, pointing to a potential mechanistic specificity of FARs. We found that even a one-time dose of recombinant FAR has severe adverse effects on the outcomes of a bacterial infection. Flies generally exhibited a decrease in survival in a dose-dependent manner, beginning with a 50 ng dose of FAR-1. During a bacterial infection the host is harmed by two factors: the pathogen and the immune response. In experiments with FAR-2, low doses (20 ng and 50 ng) led to significantly improved survival, which we hypothesize is due to the suppression of immune-induced damage. Although 250 ng is likely greater than physiological concentrations of FAR during EPN infections, it is remarkable that such a phenotype was observed with only a single component of a complex array of venom proteins found in ESPs, where hundreds of proteins usually act in concert to dampen host immunity. Interestingly, FARs not only modulate measurable outputs of immunity but affect the outcome of infection.

A key component of understanding how nematodes utilize FARs to dampen host immunity is to understand the mechanism underlying their interactions with immune molecules. We hypothesize that FARs bind to lipids that function as signaling molecules for a diverse range of functions including inflammation, immunity, homeostasis and reproduction. It has been proposed that most terrestrial insects lack free long-chain polyunsaturated fatty acids (LC-PUFAs) including arachidonic acid (AA), due to its role in oxidative stress (Chandra Roy et al., 2019; Stanley and Kim, 2018). Insects have high levels of reactive oxygen species (ROS), such as the superoxide anion (O_2^-), due to their significant production of

ATP in the mitochondrial electron transport chain. These ROS can escape the mitochondria and often react with AA and other LC-PUFAs causing lipid peroxidation leading to damaged cell membranes and possible adduct formation to proteins and nucleic acids, giving rise to additional cell damage (Chandra Roy et al., 2019; Shen et al., 2010; Stanley and Kim, 2018). In mammals, free AA is released when phospholipase A_2 (PLA_2) cleaves phospholipids directly from the membrane. In insects however, PLA_2 has been predicted to yield free linoleic acid (LA) which is then elongated to AA and subsequently converted to downstream lipids such as prostaglandins and leukotrienes that are essential signaling molecules in the immune response (Figure 6) (Stanley and Kim, 2018; Stanley et al., 2009). Our untargeted metabolomics study revealed that phosphatidylcholine (PC) and phosphatidylethanolamine (PE) were reduced in FAR expressing flies (Figure S7). These are essential phospholipids usually incorporated into the cell membrane that give rise to many downstream lipids that could have diverse functions including immune signaling and regulation (Shrestha et al., 2010). We hypothesize that they are depleted by a compensatory mechanism where more phospholipid is cleaved from the membrane and converted to downstream fatty acids that are likely sequestered and depleted more readily by FARs. Interestingly, our metabolite study of hemolymph shows a low but measurable concentration of AA, with much higher concentrations of C:18 fatty acids including oleic and linoleic acids. These data support the hypothesis that in insects, LA is cleaved directly from the lipid bilayer, providing evidence for the linoleic-to-arachidonic model of C20 biosynthesis in insects. Our data also show that FAR binds tightly to LA and not AA, *in vitro*. We hypothesize that LA is not depleted by FAR due to PLA_2's ability to readily cleave LA from the membrane and rather that FAR is inhibiting AA and its downstream products. In mammals, pro- and anti- inflammatory lipids are produced from identical precursors with the enzymes from each branch competing for substrate (Serhan et al., 2008; Wall et al., 2010). Therefore, the regulation of enzyme availability decides the outcome of the immune response. Interestingly, PLA_2 is turned on by the Toll and Imd pathways in *D. melanogaster* and inhibited by the bacterial symbionts of EPNs, *Xenorhabdus* and *Photorhabdus* (Figure 6) (Aymeric et al., 2010; Hwang et al., 2013; Kim et al., 2017; Shrestha et al., 2010). It is possible that in *Drosophila* a similar network for substrate and enzyme availability takes place, however the identity of pro- and anti-immune lipid signaling molecules is yet to be determined in this model.

Lipid signals have important roles in mammalian immunity and have been hypothesized to play similar roles in insect immune defenses (Stanley, 2006). We found that Sc-FARs bind to LA and oxidized metabolites of LA *in vitro*, which may suggest their preferred *in vivo* binding partners. Our metabolomics studies showed that arachidonic acid, 9(10)- and 12(13)-EpOME, and 13-HODE, which are known to modulate diverse physiological functions in mammals and have been shown to regulate immunity in insects (Vatanparast et al., 2020). 13-HODE has anti-inflammatory functions in mammalian immunity and is often increased under oxidative stress triggered during a disease response, are depleted in the hemolymph of FAR expressing flies (Thompson et al., 2005; Vangaveti et al., 2010). During a mammalian immune response, 9(10)- and 12(13)-EpOME are activated by and interact with inflammatory leukocytes or neutrophils (Thompson et al., 2005). These data support the hypothesis that FARs modulate host immunity by binding to the oxidation products of LA or its upstream precursors to dampen the immune response (Figure 6). While little is known about how nematodes use FARs and other ES molecules to interact with host immunity, model systems continue to be invaluable in elucidating functional activity and yielding hypotheses that can be further tested.

In summary, this study shows that FAR-1 and FAR-2 dampen the host immune response and provides evidence that nematodes likely utilize other ESPs in conjunction with FARs to modulate host immunity. We hypothesize that FARs act by disrupting lipid signaling necessary for immune responses. Deepening our understanding of how nematode parasites evade or suppress host defenses is key to further our development of treatment options for these infections.

Methods

Fly stock/ maintenance

All fly strains were grown on D2 glucose medium from Archon Scientific (Durham, North Carolina) and kept at 25°C with 50% humidity on a 12h light 12h dark cycle.

Plasmid design and assembly

To assemble plasmid OA-1010, the base vector used for generating FAR protein-expressing plasmids, several components were cloned into the piggyBac plasmid OA959C (Addgene #104968) using Gibson assembly/EA cloning. Plasmid OA959C was digested with AvrII and NotI, and the following components were cloned in with EA cloning: an*attP* sequence amplified from plasmid M{3xP3-RFP attP} with primers 1010.C1 and 1010.C2, a 10xUAS promoter fragment amplified with primers 1010.C3 and 1010.C4 from Addgene plasmid 78897, a p10 3'UTR fragment amplified from Addgene plasmid #100580 with primers 1010.C5 and 1010.C6, and opie2-dsRed marker fragment amplified from Addgene plasmid #100580 using primers 1010.C7 and 1010.C8. The resulting plasmid was then digested with XhoI and PacI, and the coding sequences (CDSs) of various FAR proteins that were codon-optimized for *D. melanogaster* expression and synthesized (GenScript, Piscataway, NJ) were separately cloned in to generate the six final FAR protein-expressing vectors. Specifically, to generate vector OA-1010Av2, the codon optimized CDS of *S. carpocapsae* gene L596_g9608 was amplified with primers 1010.C9 and 1010.C10 from a gene-synthesized plasmid and cloned into the above digested vector using EA cloning. Then, to generate vector OA-1010A, OA-1010Av2 was digested with PacI and a G(4)S linker followed by a 30-amino-acid human influenza hemagglutinin (HA) epitope tag was amplified with primers 1010.C11 and 1010.C12 from the *ninaE*[SBP-His] vector and cloned into the above digested vector using EA cloning. To generate vector OA-1010Bv2, the codon optimized CDS of *S. carpocapsae* gene L596_g25050 were amplified with primers 1010.C13 and 1010.C14 from a gene-synthesized plasmid and cloned into the digested OA-1010 vector using EA cloning. Then, to generate vector OA-1010B, OA-1010Bv2 was digested with PacI and a G(4)S linker followed by a 30-amino-acid human influenza HA epitope tag was amplified with primers 1010.C15 and 1010.C12 from the *ninaE*[SBP-His] vector and cloned into the above digested vector using EA cloning. To generate vector OA-1010C, a fragment containing the codon optimized CDS of *C. elegans* gene *far-8* followed by a G(4)S linker and a 30-amino-acid human influenza HA epitope tag was amplified with primers 1010.C16 and 1010.C12 from a gene-synthesized plasmid and cloned into the XhoI/PacI-digested OA-1010 vector using EA cloning. To generate vector OA-1010D, a fragment containing the codon optimized CDS of *A. ceylanicum* gene *Ac-far-1* (maker-ANCCEYDFT_Contig87-pred_gff_fgenesh-gene-3.1) followed by a G(4)S linker and a 30-amino-acid human influenza HA epitope tag was amplified with primers 1010.C17 and 1010.C12 from a gene-synthesized plasmid and cloned into the XhoI/PacI-digested OA-1010 vector using EA cloning. All primers used for cloning are listed in Supplementary Table xx. All codon optimization was done by GenScript (Piscataway, NJ) using OptimumGene™ algorithms.

Fly transgenesis

Transgenic flies were developed using codon optimized Sc-FAR-1 or Sc-FAR-2 inserted via the PhiC31 site-specific serine integrase method. The transgenic UAS lines were then crossed with several Gal4 drivers from the Bloomington *Drosophila* Stock Center (BDSC), including TubP-Gal4 (#5138; strong, ubiquitous somatic expression), CG-Gal4 (#7011; expressed in the fat body, hemocytes and lymph gland) and He-Gal4 (#8699; expressed in hemocytes). Fly husbandry and crosses were performed under standard conditions at 25°C. Rainbow Transgenics (Camarillo, CA) carried out all of the fly injections. All constructs were inserted into *attP* line 86Fa (BDSC #24486: y[1] M{vas-int.Dm}ZH-2A w[*]; M{3xP3-RFP.attP'}ZH-86Fa).

Western Blot

A modified version of the abcam general western blot protocol was used. 30 adult HA-tagged transgenic flies were ground up in 200 µL lysis buffer and centrifuged at 20,000g for 20 minutes at 4°C. The supernatant protein concentration was normalized to 1-2 mg/mL. 20 µL anti-HA magnetic beads (Thermo Scientific 88836) were incubated with 150 µL of supernatant protein sample while shaking for 30 minutes. The sample was then removed, and the beads were washed twice with 300 µL of TBST. The beads were then resuspended in 30 µL Tris-Cl pH 8.0 and 10 µL loading buffer. The samples were heated for 10 minutes at 100°C and electrophoresed on the SDS-PAGE gel. The proteins were transferred onto the immobilon P^{SQ} (Millipore) for 1.5 hours at 50 Volts. The membrane was washed with PBS and blocked with 1% BSA for 30 minutes with shaking. The membrane was washed twice with PBST for 10 minutes and then incubated with HA-tag primary anti-rabbit antibody (Abcam ab236623) for 2 hours with shaking. After incubation, the membrane was washed twice again with PBST for 10 minutes. Then anti-rabbit anti-goat antibody (Abcam ab6721) was added and incubated for 2 hours with shaking. Again, the membrane was washed twice with PBST and then developed with Metal enhanced DAB substrate kit (Thermo Scientific 34065).

Bacterial stock maintenance

Streptococcus pneumoniae was grown by shaking in glass vials with 5 mL tryptic soy (TS) broth (Difco TS broth, catalase, streptomycin) at 37°C with 5% CO_2 overnight. The overgrown culture was diluted in catalase (100 µL) and TS to yield a final volume of 20 mL in a flask and incubated shaking until the OD_{600} ~ 0.4 (about 1 hour). The culture was then diluted again to a final volume of 50 mL, with 150 µL catalase, and incubated until the OD_{600} ~ 0.2 - 0.4 (above 0.5 is no longer in log phase). 5% glycerol was added to the final culture and stored then in 1mL aliquots at -80°C. To use the aliquots, one tube was thawed, spun down at 14,000 rpm for 5 minutes, the supernatant was removed, and the pellet was resuspended in the desired amount of PBS (50 - 60 µL yields ~ 100,000 CFUs) and serially diluted to yield the appropriate CFU doses. For quantification of CFUs, *S.p.* was plated on TSA agar plates supplemented with 50 mL/L sheep's blood. *Listeria monocytogenes* (serotype 4b, 19115, (ATCC, VA)) was also grown in batches in brain heart infusion (BHI) medium at 37°C in aerobic condition. Cultures were grown overnight in a flask inoculated with a fresh colony and rediluted under log phase (below OD_{600} ~ 0.2) and grown up to the desired OD_{600} (~0.4). The entire volume was transferred to a 50mL centrifuge tube for vortexing. Before freezing, a 5% glycerol solution was added to the culture and 1mL aliquots were stored at -80°C. To use the aliquots, one tube was thawed, spun down at 14,000 rpm for 5 minutes, the supernatant was removed, and the pellet was resuspended in the desired amount of PBS (90 - 100 µL yields ~ 100,000 CFUs) and serially diluted to yield the appropriate CFU doses. For quantification of CFUs,*L.m.* was plated on BHI plates. *Xenorhabdus innexi* (HGB2121 *att*Tn*7*/Tn*7*-GFP (from pURR25)) was incubated at 27°C shaking in Luria Bertani (LB) broth supplemented with 0.1% sodium pyruvate (sp). Overnight cultures on *X. innexi* were subcultured below log phase (OD_{600}< 0.4) and grown back to log phase (OD_{600} 0.4 - 0.8) and diluted to the desired concentrations before use, as well as streaked on LB+sp plates bi-weekly for storage. LB+sp media was supplemented with 20% glycerol for long term storage of log phase *X. innexi* in -80°C.

Generation of recombinant proteins

The sequence corresponding to *Sc*FARS-1 *and Sc*FARS-2 was obtained from GenBank (Benson et al., 2013).The sequences encoding the mature protein was codon-optimized, synthesized by GenScript and cloned into a modified pET28 vector incorporating an N-terminal hexahistidine tag and a TEV cleavage site. *Sc*FARS-1 *and Sc*FARS-2 were produced recombinantly in *E. coli* BL21-CodonPlus cells (Stratagene) grown in autoinduction medium (Invitrogen) from a 1% inoculum. Following four hours of growth at 37°C and 16 hours at 30°C, the cells were harvested, and the pellet resuspended in 20 mM Hepes pH 8.3, 1 M NaCl, 30 mM imidazole. Cells in suspension were lysed using a French press, insoluble material was removed by centrifugation, and the soluble fraction was applied to a HisTRAP FF 5 mL column (GE Healthcare). Bound *Sc*FARs1 and 2 were eluted with an increasing concentration of imidazole, the His tag was subsequently removed by TEV cleavage, and they were further purified by gel filtration chromatography on a Superdex 200 16/60 HiLoad column in HBS (20 mM Hepes pH 7.5, 150 mM NaCl). The purity of was assessed at each stage by SDS-PAGE.

Fly injections, survival and CFUs

For injections and immune assays, 5-7-day-old male flies were anesthetized with CO_2 and injected with various CFU doses yielding a total volume of 50 nL precisely using a MINJ-FLY high-speed pneumatic injector (Tritech Research, CA) and individually pulled calibrated glass needles. Flies were injected into the abdomen close to where the thorax meets and slightly ventral from the dorsal-ventral cuticle axis, easily visible below the haltere. Survival studies were carried out for all of the pathogens we tested. After injection of the CFU dose or phosphate buffered saline (PBS) control, flies were placed in vials in groups of 30 with a total of 60 flies per experimental or control group. Flies injected with the human pathogens (*S.p.* and *L.m.)* were kept at 28°C with 50% humidity compared to flies injected with the insect pathogen *X.i.* which was kept at 25°C with 50% humidity. The number of dead flies was counted daily and Kaplan-Meier survival curves were generated with GraphPad Prism software with statistics shown as log-rank analysis (Mantel-Cox). Survival experiments were at least triplicated. CFUs were determined by homogenizing a single infected, or buffer-injected fly in 200 µL of PBS, serially diluted and plated on the appropriate agar plates and incubated overnight. Colonies were counted the next day. At least five flies per condition were homogenized for CFU quantification each time an injection experiment was done to measure time 0 CFUs which are representative of all fly strains. All fly strains were injected at the same

time for each experimental replicate. Using GraphPad Prism software, results are shown as scatter plots with statistical significance analyzed using an unpaired t-test.

PO & disseminated melanization

Flies were injected with 1,000 CFUs of *L. monocytogenes* to elicit an immune induced melanization cascade. Phenoloxidase activity was measured as previously described (Binggeli et al., 2014; Cooper et al., 2019). To collect hemolymph, 20-30 flies 4 hours post injection (p.i.) were pricked through the thorax and placed in a pierced 0.5 µL Eppendorf tube and covered with glass beads, then placed inside a 1.5 µL Eppendorf tube containing 30 µL of 1x protease inhibitor cocktail (Fisher, PI78429). Samples were centrifuged at 10,000 rpm for 20 minutes at 4°C. Protein concentrations were measured with Bradford assay (Bio-rad, 5000006) and then diluted in phosphate buffered saline (PBS) to a concentration of 15 µg/uL and a total volume of 100 µL. Using a clear 96-well plate, each well contained 160 µL L-Dopa (3 mg/mL) dissolved in phosphate buffer (37.5% 1 M potassium phosphate, 62.5% 1 M sodium phosphate, pH 6.5), 35 µL of hemolymph sample and 5 µL $CaCl_2$ (20 mM). PO activity was measured by kinetic reads at 29°C at 492 nm every minute for 60 min with 5 seconds of shaking between reads. The OD of a blank control was subtracted from all biological values. Experiments were replicated five times with three technical replicates per experiment. Data were plotted as mean+SEM by taking the peak OD value (timepoint ~ 30 min). Statistics shown as an unpaired t-test was done in GraphPad Prism. For disseminated melanization, flies were observed for melanin deposits in the posterior and anterior abdomen, thorax, head and eyes four days p.i. with *L.m.* An individual was considered to show disseminated melanization if it had two or more deposits of melanin, one often at the wounding site and another either underneath the cuticle or in deeper tissues as previously described (Ayres and Schneider, 2008). Data were graphed as percent of the population infected that was melanized by day four p.i. as the mean+SEM. Experiments were replicated three times with 40 individuals per experimental condition per experiment. Statistics shown as unpaired t-test was done in GraphPad Prism.

Antimicrobial peptide gene expression - qPCR

Total RNA was extracted from 15 *S. pneumonia* infected flies per strain 24 hours post-injection using Trizol reagent (Molecular Research Center, Inc; Cincinnati, Ohio) according to the manufacturer instructions. Integrity of RNA was confirmed by observing bands on an agarose gel and concentration was determined by nanodrop. Reverse transcription of RNA using ProtoScript II First Strand cDNA synthesis kit (New England BioLabs, NE, E6560L) following the manufacturer protocol, in a MultiGene OptiMax Thermal Cycler (Labnet international, NJ). The qRT-PCR was done with a CFX Connect Bio-Rad system with Perfecta SYBR green supermix (QuantaBio, MA) and gene specific primers for *Defensin, Drosomycin*, and *Tubulin* (Integrated DNA Technologies, IA). Experiments were carried out with three technical replicates and repeated four times with plots shown as bar graphs with individual points representing each replicate. Statistics shown as One-way ANOVA done in GraphPad Prism.

In vitro binding -

The fatty acid- and retinol- binding preferences of Sc-FAR *in vitro* was measured by utilizing the saturated fatty acid fluorescent probe 11-(Dansylamino) undecanoic acid (DAUDA) (Sigma-Aldrich, USA) and retinol as previously described (Fairfax et al., 2009; Kennedy et al., 1997). Fluorescent emission spectra for Sc-FAR bound to DAUDA (1 µM) and retinol (40 µM) were measured at 25°C in a black-walled 96-well plate yielding a total volume of 200 µL with an excitation wavelength of 345 nm and 350 nm respectively. When DAUDA is encompassed by a binding protein a 50nm blue shift is observed with an excitation wavelength of 345nm. The equilibrium dissociation constant (Kd) for Sc-FAR bound to DAUDA or retinol was estimated by adding increasing concentrations of Sc-FAR, in 1 or 2 µM increments, to 1 µM DAUDA in PBS and 40 µM retinol in PBS. The data were normalized to the peak fluorescence intensity of DAUDA or retinol bound to FAR (yielding a value of 1) and corrected for background fluorescence of PBS alone for each concentration. The data were then plotted as relative fluorescence and a nonlinear fit via the one site-specific system was used to find the Kd value in GraphPad Prism. Competition studies were done by measuring the decrease in peak emission of DAUDA in the presence of another fatty acid in 10-fold excess. Oleic, linoleic and arachidonic acid were tested along with 9,(10)- and 12,(13)- EpOME and 13-HODE(Cayman Chemicals, MI). All competition experiments were replicated 3 times with 3 technical replicates per experiment, plotted as bar graphs with mean+SEM and individual points for each replicate, analyzed by an unpaired t-test. All fatty acids and DAUDA were stored in -20°C and freshly diluted before

each experiment starting with a working solution of either 10 or 100 µM in 100% ethanol and then subsequently diluted in PBS to achieve the appropriate working solution.

Metabolomics

Whole fly untargeted -

Flies were transferred to a 2 mL bead mill tube and weighed, the range was 131 mg to 302 mg. Ice-cold extraction solvent (20:20:30:30 water:IPA:ACN:MeOH) was added, 3.32 µL / 1 mg sample, and samples were homogenized in a liquid nitrogen cooled bead mill, 6, 10 s cycles at 5 m/s. After centrifugation for 15 min at 16,000 x g at 4 C, the supernatant was analyzed by LC-MS. LC-MS metabolomics analysis was performed at the UC Riverside Metabolomics Core Facility as described previously (Rothman et al., 2019). Briefly, analysis was performed on a Synapt G2-Si quadrupole time-of-flight mass spectrometer (Waters) coupled to an I-class UPLC system (Waters). Separations were carried out on a CSH phenyl-hexyl column (2.1 x 100 mm, 1.7 µM) (Waters). The mobile phases were (A) water with 0.1% formic acid and (B) acetonitrile with 0.1% formic acid. The flow rate was 250 µL/min and the column was held at 40° C. The injection volume was 2 µL in positive ion mode and 4 µL in negative ion mode. The gradient was as follows: 0 min, 1% B; 1 min, 1% B; 8 min, 40% B; 24 min, 100% B; 26.5 min, 100% B; 27 min, 1% B. The MS was operated in positive ion mode (50 to 1200 m/z) with a 100 ms scan time. MS/MS was acquired in data dependent fashion. Source and desolvation temperatures were 150°C and 600°C, respectively. Desolvation gas was set to 1100 L/hr and cone gas to 150 L/hr. All gases were nitrogen except the collision gas, which was argon. Capillary voltage was 1 kV in positive ion mode and 2 kV in negative ion mode. A quality control sample, generated by pooling equal aliquots of each sample, was analyzed every 4-6 injections to monitor system stability and performance. Samples were analyzed in random order. Leucine enkephalin was infused and used for mass correction. Untargeted data processing (peak picking, alignment, deconvolution, integration, normalization, and spectral matching) was performed in Progenesis Qi software (Nonlinear Dynamics). Data were normalized to total ion abundance. To aid in the identification of features that belong to the same metabolite, features were assigned a cluster ID using RAMClust (Broeckling et al., 2014). An extension of the metabolomics standard initiative guidelines was used to assign annotation level confidence (Schymanski et al., 2014; Sumner et al., 2007). Annotation level 1 indicates a match to an in-house library. Level 2a indicates an MS and MS/MS match to an external database. Level 2b indicates an MS and MS/MS match to the Lipiblast in-silico database (Kind et al., 2013) or an MS match and diagnostic evidence, such as the dominant presence of an m/z 85 fragment ion for acylcarnitines. Level 3 indicates an MS and partial MS/MS match to an external or in-house database. Several mass spectral metabolite databases were searched against including Metlin, Mass Bank of North America, and an in-house database. Statistical analyses were performed, and figures generated using R.

Hemolymph only (WashU) -

Hemolymph from 200 5-7-day old male flies was extracted as previously described in (Kwon et al., 2015). Briefly, flies were pierced through the thorax with a tungsten needle. Flies were placed in a pierced 0.5 mL Eppendorf tube within a 1.5 mL Eppendorf tube containing 20µL of 10x protease inhibitor cocktail and centrifuged for two rounds of 10 minutes at 10,000 rpm at 4°C with a gentle mixing in between rounds. The supernatant of the collected hemolymph was centrifuged for 10 minutes at 14,000 rpm to remove cells and debris. The supernatant was flash-frozen in liquid nitrogen and stored at -80°C until prepped for metabolomics experiments. Each of the pooled drosophila samples was initially homogenized with 250 µL of PBS buffer. Arachidonic acid (AA) was extracted from 50 µL of the homogenate with 200 µL of methanol, containing 10 ng of deuterated AA-d8 as the internal standard. Both endogenous and deuterated AA were derivatized with dimethylaminoprpylamine (DMAPA) for improving MS detection of these compounds. PGE2 and 5-HETE were extracted from another aliquot of the homogenate (50 µL) with 200 µL of methanol, containing 2 ng each of their deuterated standards. Three-point calibration standards of AA, PGE2, and 5-HETE
containing their deuterated internal standards were also prepared for the absolute quantification. The sample analysis was performed with a Shimadzu 20AD HPLC system coupled to a tandem mass spectrometer (API-6500+Qtrap: Applied Biosystems) operated in MRM mode. The positive ion ESI mode was used for detection of AA and AA-d8 and the negative ion ESI was used for detection of PGE2 and 5-HETE as well as their deuterated standards. All samples were injected in duplicate for data averaging. Data processing was conducted with Analyst 1.6.3 (Applied Biosystems). Metabolomic

analysis of fly hemolymph was performed by the Metabolomics Facility of Washington University (St. Louis, MI).

Statistics

All statistics were done with GraphPad Prism 8.4. Statistical significance indicated with asterisks indicating the following p-value cut offs: 0.05-0.033*, 0.033-0.002**, 0.002-0.0002*** and <0.0001****.

Acknowledgements

We thank Joshua Mallilay, Nikhil Prabhakar, and Priscila Robles, for their assistance with experimentation, fly husbandry and maintenance, and Bloomington *Drosophila* Stock Center (NIH P40 OD018537) for providing fly stocks. We thank Jay Kirkwood and the UC Riverside Metabolomics Core Facility, and the Metabolomics Facility at Washington University for their assistance with parts of this study. This research was supported by a USDA National Institute of Food and Agriculture Hatch project (accession #1015192) and R35 GM137934 National Institute of General Medical Sciences to A.R.D. and by a Canadian Institutes of Health Research Grants 148596 to M.J.B. M.J.B. gratefully acknowledges the Canada Research Chair program for salary support. O.S.A and A.B. were supported in part by UCSD startup funds.

References

Aymeric, J.L., Givaudan, A., and Duvic, B. (2010). Imd pathway is involved in the interaction of Drosophila melanogaster with the entomopathogenic bacteria, Xenorhabdus nematophila and Photorhabdus luminescens. Mol Immunol *47*, 2342-2348.

Ayres, J.S., and Schneider, D.S. (2008). A signaling protease required for melanization in Drosophila affects resistance and tolerance of infections. PLoS Biol *6*, 2764-2773.

Bath, J.L., Robinson, M., Kennedy, M.W., Agbasi, C., Linz, L., Maetzold, E., Scheidt, M., Knox, M., Ram, D., Hein, J.*, et al.* (2009). Identification of a Secreted Fatty Acid and Retinol-Binding Protein (Hp-FAR-1) from Heligmosomoides polygyrus. Journal of Nematology *41*, 228-233.

Benson, D.A., Cavanaugh, M., Clark, K., Karsch-Mizrachi, I., Lipman, D.J., Ostell, J., and Sayers, E.W. (2013). GenBank. Nucleic Acids Res *41*, D36-42.

Binggeli, O., Neyen, C., Poidevin, M., and Lemaitre, B. (2014). Prophenoloxidase activation is required for survival to microbial infections in Drosophila. PLoS Pathog *10*, e1004067.

Bradley, J.E., Nirmalan, N., Kläger, S.L., Faulkner, H., and Kennedy, M.W. (2001). River blindness: a role for parasite retinoid-binding proteins in the generation of pathology? Trends in Parasitology *17*, 471-475.

Broeckling, C.D., Afsar, F.A., Neumann, S., Ben-Hur, A., and Prenni, J.E. (2014). RAMClust: a novel feature clustering method enables spectral-matching-based annotation for metabolomics data. Anal Chem *86*, 6812-6817.

Castillo, J.C., Reynolds, S.E., and Eleftherianos, I. (2011). Insect immune responses to nematode parasites. Trends Parasitol *27*, 537-547.

Chandra Roy, M., Lee, D., and Kim, Y. (2019). Host Immunosuppression Induced by Steinernema feltiae, an Entomopathogenic Nematode, through Inhibition of Eicosanoid Biosynthesis. Insects *11*.

Ciche, T. (2007). The biology and genome of Heterorhabditis bacteriophora. WormBook, 1-9.

Cooper, D., and Eleftherianos, I. (2016). Parasitic Nematode Immunomodulatory Strategies: Recent Advances and Perspectives. Pathogens *5*.

Cooper, D., Wuebbolt, C., Heryanto, C., and Eleftherianos, I. (2019). The prophenoloxidase system in Drosophila participates in the anti-nematode immune response. Mol Immunol *109*, 88-98.

Dillman, A.R., Macchietto, M., Porter, C.F., Rogers, A., Williams, B., Antoshechkin, I., Lee, M.M., Goodwin, Z., Lu, X., Lewis, E.E.*, et al.* (2015). Comparative genomics of Steinernema reveals deeply conserved gene regulatory networks. Genome Biol *16*, 200.

Fairfax, K.C., Harrison, L.M., and Cappello, M. (2014). Molecular cloning and characterization of a nematode polyprotein antigen/allergen from the human and animal hookworm Ancylostoma ceylanicum. Mol Biochem Parasitol *198*, 37-44.

Fairfax, K.C., Vermeire, J.J., Harrison, L.M., Bungiro, R.D., Grant, W., Husain, S.Z., and Cappello, M. (2009). Characterisation of a fatty acid and retinol binding protein orthologue from the hookworm Ancylostoma ceylanicum. Int J Parasitol *39*, 1561-1571.

Garofalo, A., Klagera, S.L., Rowlinsona, M.-C., Nirmalan, N., Klion, A., Allen, J.E., Kennedy, M.W., and Bradley, J.E. (2002). The FAR proteins of filarial nematodes: secretion, glycosylation and lipid binding characteristics. Mol Biochem Parasitol *122*, 161-170.

Hallem, E.A., Rengarajan, M., Ciche, T.A., and Sternberg, P.W. (2007). Nematodes, bacteria, and flies: a tripartite model for nematode parasitism. Curr Biol *17*, 898-904.

Hanson, M.A., Dostalova, A., Ceroni, C., Poidevin, M., Kondo, S., and Lemaitre, B. (2019). Synergy and remarkable specificity of antimicrobial peptides in vivo using a systematic knockout approach. Elife *8*.

Hoffmann, J.A., Kafatos, F.C., Jr., C.A.J., and Ezekowitz, R.A.B. (1999a). Phylogenetic Perspectives in Innate Immunity. Science *284*, 1313-1318.

Hoffmann, J.A., Kafatos, F.C., Jr., C.A.J., and Ezekowitz, R.A.B. (1999b). Phylogenetic Perspectives in Innate Immunity. Science, 1313-1318.

Hotez, P.J., Alvarado, M., Basanez, M.G., Bolliger, I., Bourne, R., Boussinesq, M., Brooker, S.J., Brown, A.S., Buckle, G., Budke, C.M.*, et al.* (2014). The global burden of disease study 2010: interpretation and implications for the neglected tropical diseases. PLoS Negl Trop Dis *8*, e2865.

Hwang, J., Park, Y., Kim, Y., Hwang, J., and Lee, D. (2013). An entomopathogenic bacterium, Xenorhabdus nematophila, suppresses expression of antimicrobial peptides controlled by Toll and Imd pathways by blocking eicosanoid biosynthesis. Arch Insect Biochem Physiol *83*, 151-169.

Iberkleid, I., Vieira, P., de Almeida Engler, J., Firester, K., Spiegel, Y., and Horowitz, S.B. (2013). Fatty acid-and retinol-binding protein, Mj-FAR-1 induces tomato host susceptibility to root-knot nematodes. PLoS One *8*, e64586.

Jordanova, R., Groves, M.R., Kostova, E., Woltersdorf, C., Liebau, E., and Tucker, P.A. (2009). Fatty acid- and retinoid-binding proteins have distinct binding pockets for the two types of cargo. J Biol Chem *284*, 35818-35826.

Kennedy, M.W., Allen, J.E., Wright, A.S., McCruden, A.B., and Cooper, A. (1995a). The gp15/400 polyprotein antigen of Brugia malayi binds fatty acids and retinoids. Mol Biochem Parasitol *71*, 41-50.

Kennedy, M.W., Brass, A., McCruden, A.B., Price, N.C., Kelly, S.M., and Cooper, A. (1995b). The ABA-1 Allergen of the Parasitic Nematode Ascaris suum: Fatty Acid and Retinoid Binding Function and Structural Characterization. Biochemistry *34*, 6700-6710.

Kennedy, M.W., Corsico, B., Cooper, A., and Smith, B.O. (2013). The unusual lipid-binding proteins of nematodes: NPAs nemFABPs and FARs. Molecular Biology, Biochemistry and Immunology *2*, 397-412.

Kennedy, M.W., Garside, L.H., Goodrick, L.E., McDermott, L., Brass, A., Price, N.C., Kelly, S.M., Cooper, A., and Bradley, J.E. (1997). The Ov20 Protein of the Parasitic Nematode Onchocerca volvulus. The Journal of Biological Chemistry *272*, 29442-29448.

Kim, I.H., Aryal, S.K., Aghai, D.T., Casanova-Torres, A.M., Hillman, K., Kozuch, M.P., Mans, E.J., Mauer, T.J., Ogier, J.C., Ensign, J.C.*, et al.* (2017). The insect pathogenic bacterium Xenorhabdus innexi has attenuated virulence in multiple insect model hosts yet encodes a potent mosquitocidal toxin. BMC Genomics *18*, 927.

Kind, T., Liu, K.H., Lee, D.Y., DeFelice, B., Meissen, J.K., and Fiehn, O. (2013). LipidBlast in silico tandem mass spectrometry database for lipid identification. Nat Methods *10*, 755-758.

Kwon, Y., Song, W., Droujinine, I.A., Hu, Y., Asara, J.M., and Perrimon, N. (2015). Systemic organ wasting induced by localized expression of the secreted insulin/IGF antagonist ImpL2. Dev Cell *33*, 36-46.

Lemaitre, B., and Hoffmann, J. (2007). The host defense of Drosophila melanogaster. Annu Rev Immunol *25*, 697-743.

Lok, J.B. (2007). Strongyloides stercoralis: a model for translational research on parasitic nematode biology. WormBook, 1-18.

Lu, D., Macchietto, M., Chang, D., Barros, M.M., Baldwin, J., Mortazavi, A., and Dillman, A.R. (2017). Activated entomopathogenic nematode infective juveniles release lethal venom proteins. PLoS Pathog *13*, e1006302.

Pullan, R.L., Smith, J.L., Jasrasaria, R., and Brooker, S.J. (2014). Global numbers of infection and disease burden of soil transmitted helminth infections in 2010. Parasites & Vectors.

Ramanathan, R., Varma, S., Ribeiro, J.M., Myers, T.G., Nolan, T.J., Abraham, D., Lok, J.B., and Nutman, T.B. (2011). Microarray-based analysis of differential gene expression between infective and noninfective larvae of Strongyloides stercoralis. PLoS Negl Trop Dis *5*, e1039.

Rey-Burusco, M.F., Ibanez-Shimabukuro, M., Cooper, A., Kennedy, M.W., Corsico, B., and Smith, B.O. (2014). (1)H, (1)(3)C and (1)(5)N chemical shift assignments of Na-FAR-1, a helix-rich fatty acid and retinol binding protein of the parasitic nematode Necator americanus. Biomol NMR Assign *8*, 19-21.

Rey-Burusco, M.F., Ibanez-Shimabukuro, M., Gabrielsen, M., Franchini, G.R., Roe, A.J., Griffiths, K., Zhan, B., Cooper, A., Kennedy, M.W., Corsico, B.*, et al.* (2015). Diversity in the structures and ligand-binding sites of nematode fatty acid and retinol-binding proteins revealed by Na-FAR-1 from Necator americanus. Biochem J *471*, 403-414.

Rothman, J.A., Leger, L., Kirkwood, J.S., and McFrederick, Q.S. (2019). Cadmium and Selenate Exposure Affects the Honey Bee Microbiome and Metabolome, and Bee-Associated Bacteria Show Potential for Bioaccumulation. Appl Environ Microbiol *85*.

Schymanski, E.L., Jeon, J., Gulde, R., Fenner, K., Ruff, M., Singer, H.P., and Hollender, J. (2014). Identifying small molecules via high resolution mass spectrometry: communicating confidence. Environ Sci Technol *48*, 2097-2098.

Serhan, C.N., Chiang, N., and Van Dyke, T.E. (2008). Resolving inflammation: dual anti-inflammatory and pro-resolution lipid mediators. Nat Rev Immunol *8*, 349-361.

Shen, L.R., Lai, C.Q., Feng, X., Parnell, L.D., Wan, J.B., Wang, J.D., Li, D., Ordovas, J.M., and Kang, J.X. (2010). Drosophila lacks C20 and C22 PUFAs. J Lipid Res *51*, 2985-2992.

Shepherd, C., Navarro, S., Wangchuk, P., Wilson, D., Daly, N.L., and Loukas, A. (2015). Identifying the immunomodulatory components of helminths. Parasite Immunol *37*, 293-303.

Shrestha, S., Park, Y., Stanley, D., and Kim, Y. (2010). Genes encoding phospholipases A2 mediate insect nodulation reactions to bacterial challenge. J Insect Physiol *56*, 324-332.

Stanley, D. (2006). Prostaglandins and other eicosanoids in insects: biological significance. Annu Rev Entomol *51*, 25-44.

Stanley, D., and Kim, Y. (2018). Prostaglandins and Other Eicosanoids in Insects: Biosynthesis and Biological Actions. Front Physiol *9*, 1927.

Stanley, D., Miller, J., and Tunaz, H. (2009). Eicosanoid actions in insect immunity. J Innate Immun *1*, 282-290.

Sumner, L.W., Amberg, A., Barrett, D., Beale, M.H., Beger, R., Daykin, C.A., Fan, T.W., Fiehn, O., Goodacre, R., Griffin, J.L.*, et al.* (2007). Proposed minimum reporting standards for chemical analysis Chemical Analysis Working Group (CAWG) Metabolomics Standards Initiative (MSI). Metabolomics *3*, 211-221.

Thompson, F.J., Mitreva, M., Barker, G.L., Martin, J., Waterston, R.H., McCarter, J.P., and Viney, M.E. (2005). An expressed sequence tag analysis of the life-cycle of the parasitic nematode Strongyloides ratti. Mol Biochem Parasitol *142*, 32-46.

Troha, K., and Buchon, N. (2019). Methods for the study of innate immunity in Drosophila melanogaster. Wiley Interdiscip Rev Dev Biol *8*, e344.

Vangaveti, V., Baune, B.T., and Kennedy, R.L. (2010). Hydroxyoctadecadienoic acids: novel regulators of macrophage differentiation and atherogenesis. Ther Adv Endocrinol Metab *1*, 51-60.

Vanha-Aho, L.M., Valanne, S., and Ramet, M. (2016). Cytokines in Drosophila immunity. Immunol Lett *170*, 42-51.

Vatanparast, M., Ahmed, S., Lee, D.H., Hwang, S.H., Hammock, B., and Kim, Y. (2020). EpOMEs act as immune suppressors in a lepidopteran insect, Spodoptera exigua. Sci Rep *10*, 20183.

Wall, R., Ross, R.P., Fitzgerald, G.F., and Stanton, C. (2010). Fatty acids from fish: the anti-inflammatory potential of long-chain omega-3 fatty acids. Nutr Rev *68*, 280-289.

Ward, J.D. (2015). Rendering the Intractable More Tractable: Tools from Caenorhabditis elegans Ripe for Import into Parasitic Nematodes. Genetics *201*, 1279-1294.

WHO (2020). Soil-transmitted helminth infections (who.int: World Health Organization).

Zhan, B., Arumugam, S., Kennedy, M.W., Tricoche, N., Lian, L.Y., Asojo, O.A., Bennuru, S., Bottazzi, M.E., Hotez, P.J., Lustigman, S.*, et al.* (2018). Ligand binding properties of two Brugia malayi fatty acid and retinol (FAR) binding proteins and their vaccine efficacies against challenge infection in gerbils. PLoS Negl Trop Dis *12*, e0006772.

Figures

	FAR encoding genes											
Spp.	*Scar*	*Acey*	*Sste*	*Alum*	*Bmal*	*Cele*	*Dmed*	*Hcon*	*Ovol*	*Nbra*	*Tspi*	*Tmur*
# of genes	45	24	16	5	3	9	3	11	3	12	0	0

Table 1: Number of putative FAR-encoding genes present in the genomes of various nematode species. Species in order from left to right: *Steinernema carpocapsae, Ancylostoma ceylanicum, Strongyloides stercoralis, Ascaris lumbricoides, Brugia malayi, Caenorhabditis elegans, Dracunculus medinensis, Haemonchus contortus, Onchocera volvulus, Nippostrongylus brasiliensis, Trichinella spiralis, Trichiuris muris*. *Trichinella spiralis* and *Trichiuris muris* have no known FAR encoding genes while *Steinernema carpocapsae* shows the greatest expansion of FAR genes in its genome.

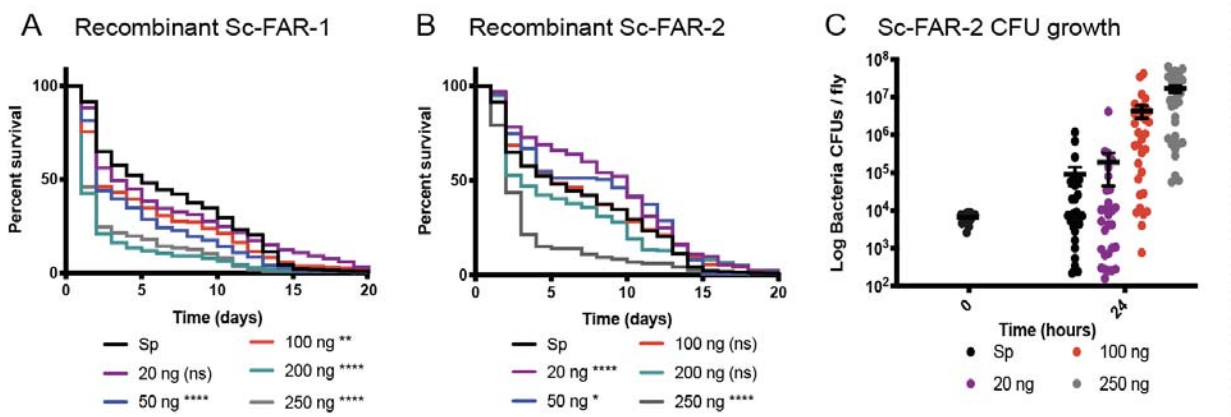

Fig 1: Recombinant FARs reduced fly survival in a dose-dependent manner. A&B) 7,000 CFUs of *S. pneumonia* (*Sp*) were co-injected with various nanogram doses of either Sc-FAR-1 or -2. C) CFUs were measured at 24 hours post-injection for panel B which shows a trend of increased bacterial growth with increasing protein doses. All controls for survival curves (black) are *Sp*-injected only, without the addition of FAR proteins. Time 0 CFUs representative of all fly strains. Log-rank test p-value significance indicated by asterisks on Kaplan Meier graphs. CFU graphs show p-value significance of an unpaired t-test (error bars show mean+SEM). Survival curves n≥180, CFU graph n≥24. All raw data available in supplemental materials.

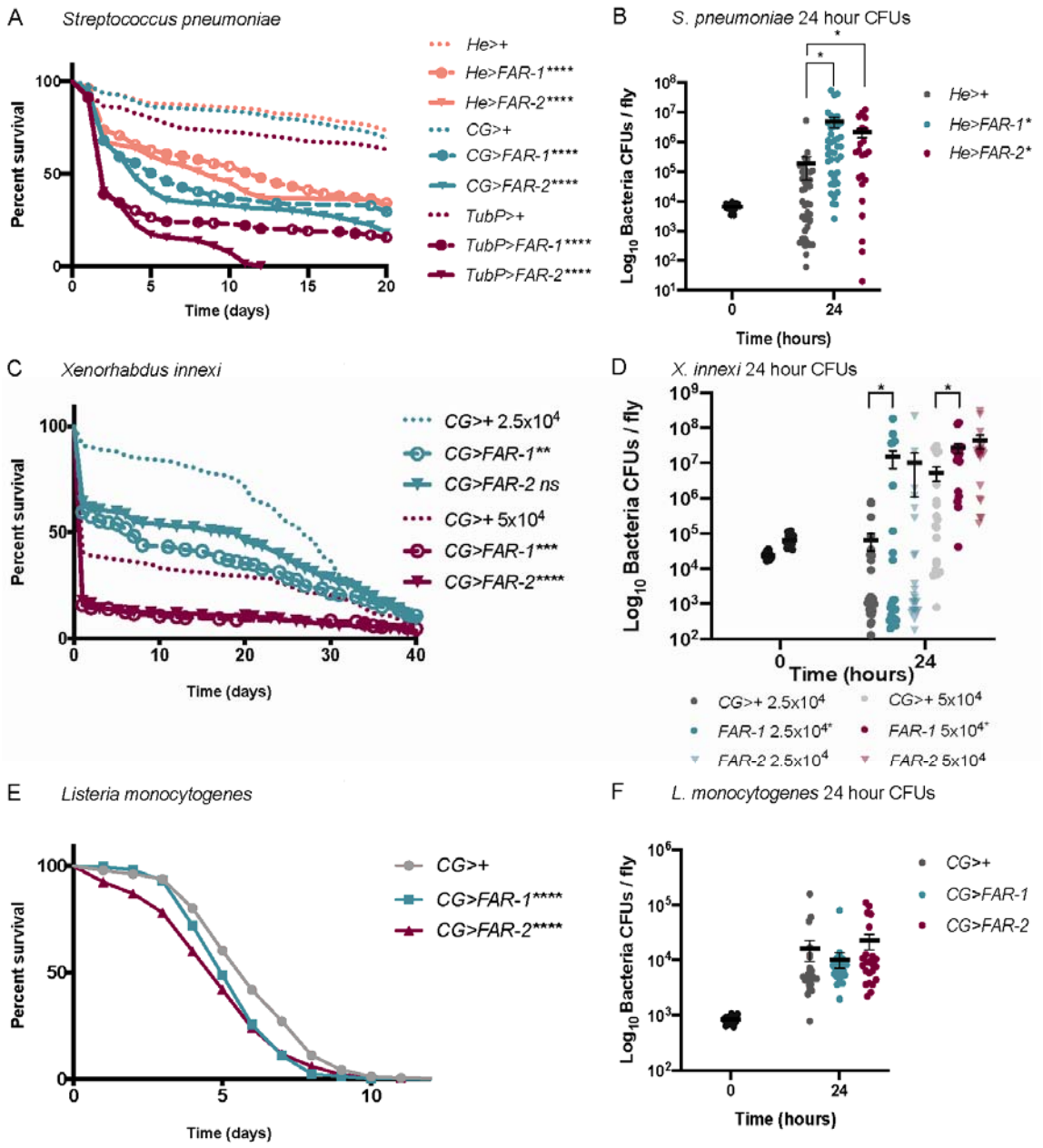

Fig 2: Transgenic FAR expression significantly decreases fly survival and increases bacterial load 24-hours post-injection. Flies were injected with specified doses of various pathogens. Survival was monitored daily and bacterial load was measured 24 hours post-injection. A&B) Flies Sc-FAR-1 & -2 expressed with a tubulin driver (TubP), a fat body, hemocyte and lymph gland specific driver (CG), and a hemocyte only driver (He) were injected with 7,000 CFUs of *Streptococcus pneumoniae*. Survival curves of flies are shown in (A) and bacterial CFUs in the He driver flies at 24-hour post injection in (B). C&D) Flies with Sc-FAR-1 & -2 expression with the CG driver were injected with 25,000 and 50,000 CFUs (shown at time 0) of *Xenorhabdus innexi*. Survival curves of flies are shown in (C) and bacterial CFUs in (D). E&F) Flies with Sc-FAR-1 & -2 expression with the CG driver were injected with 1,000 CFUs of *Listeria monocytogenes*. Survival curves of flies are shown in (E) and bacterial CFUs in (F). All controls are 86Fa flies crossed with flies containing the specified driver. Time 0 CFUs representative of all fly strains (depicted in black). Statistics shown as log-rank test p-value for survival curves and unpaired t-test for microbe growth with (error bars show mean+SEM). Survival curves n≥180, CFU graph n≥24 over at least 3 experiments. All raw data available in supplemental materials.

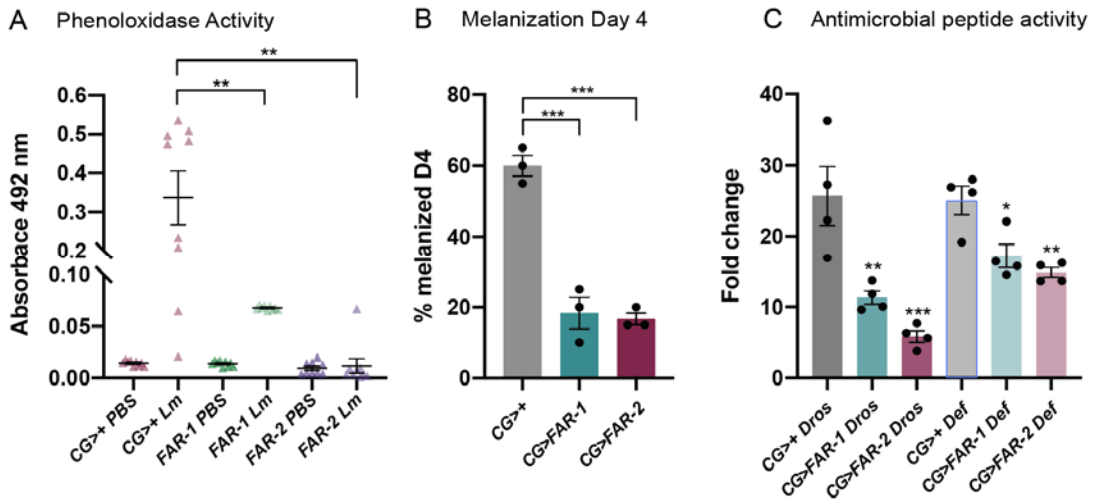

Fig 3: Melanization, phenoloxidase and antimicrobial peptide activity was diminished in FAR expressing flies. A) Flies were injected with the LD_{30} of *L. monocytogenes* (1,000 CFUs) and phenoloxidase activity was measured 6 hours post-injection. B) Flies were injected with the LD_{30} of *L. monocytogenes* and disseminated melanization was observed 4 days post-injection. C) 24 hours post-injection with the LD_{30} dose of *S. pneumoniae* the relative increase in the antimicrobial peptides (AMP) *Drosomycin* (Toll) and *Defensin* (Imd) were analyzed. Compared to the CG>+ control, FAR-1 and -2 significantly suppress both AMPs. Four experiments were completed with 15 flies per experimental group. Asterisks indicate statistical significance from one-way ANOVA (A & C) and unpaired t-test (B). All experiments were repeated at least 3 times, error bars show mean+SEM. All raw data available in supplemental materials.

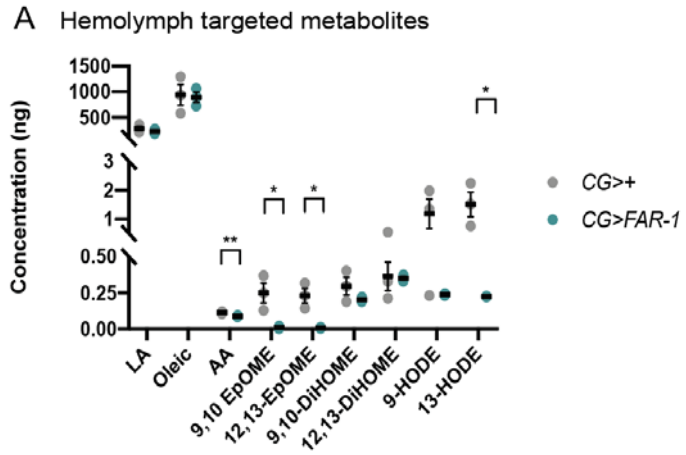

Fig 4: Metabolite abundance in FAR expressing and control hemolymph. A) Fly hemolymph samples were analyzed for abundance of various lipids. 9(10)- and 12(13)- EpOME, 9- and 13-HODE and arachidonic acid were depleted in FAR-1 expressing flies. Statistics shown as an unpaired t-test and error bars show mean+SEM. All raw data available in supplemental materials.

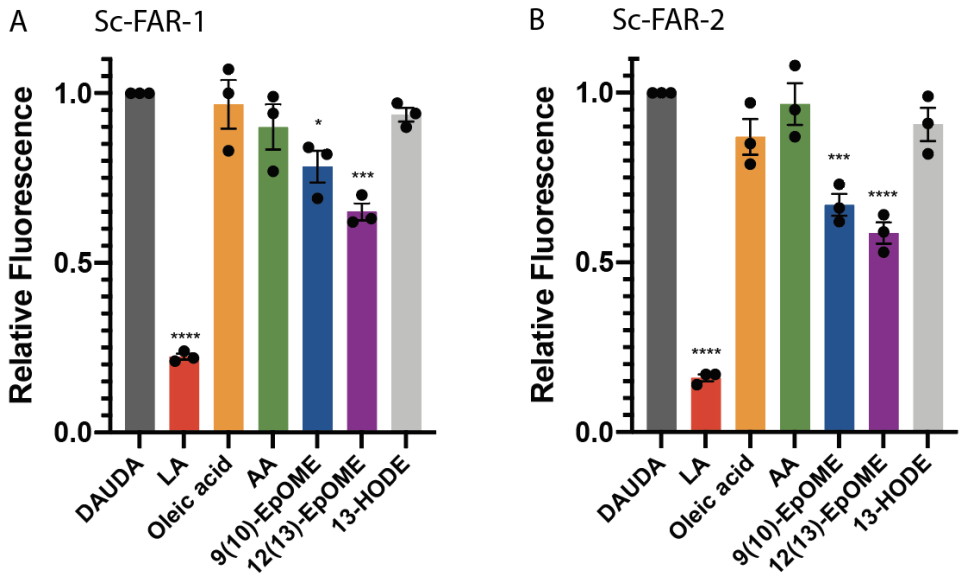

Fig 5: In vitro binding of Sc-FARs. A&B) Competitive binding between 10-fold excess linoleic (LA), oleic, arachidonic (AA) acid, and other fatty acids (all 10 µM) and DAUDA (1 µM) was tested in the context of FAR-1 & 2. Linoleic acid displaces DAUDA the most, as seen by the largest reduction in relative fluorescence. Both 9(10)- and 12(13)-EpOME displace DAUDA more easily in the presence of FAR-2, showing tighter binding. Statistics shown as One-way ANOVA and error bars show mean+SEM. All raw data available in supplemental materials.

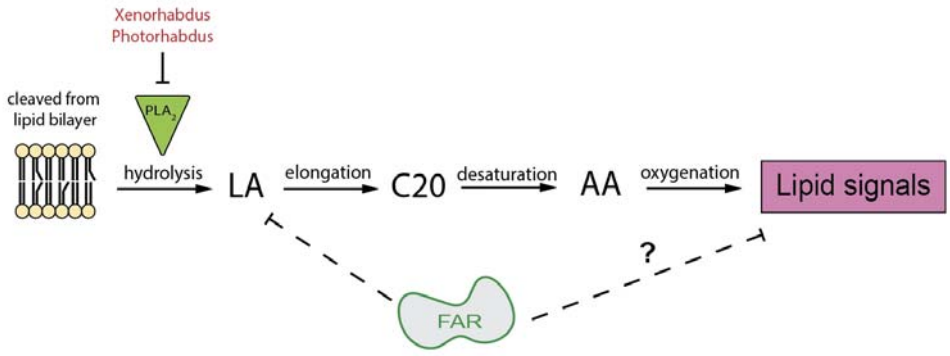

Fig 6: Key components of lipid biosynthesis in insects. Our hypothesis is that FARs are sequestering essential fatty acids and/or their upstream lipids to disrupt lipid signaling that is necessary for certain host immune functions. We have shown FARs' ability to bind to L*A in vit*ro which could temporarily disrupt downstream eicosanoid signaling. In insects, phospholipase A2 cleaves linoleic acid (LA) from the lipid bilayer instead of arachidonic acid in mammals. Free LA is then extended via an elongase to a C20 fatty acid. Desaturase oxidizes the C20 to arachidonic acid which can then be oxygenated to yield eicosanoid-like molecules. Eicosanoids are involved in many important functions including gene expression, immune regulation and reproduction. Adapted (Stanley and Kim, 2018).